TEMPERED LOCAL ENSEMBLE TRANSFORM KALMAN FILTER: SIMPLE MODEL EXPERIMENTS

Jorge Gacitúa Gutiérrez[1,2 *], Juan Ruiz[1,2,3], Manuel Pulido[4], Maria Eugenia Dillon[5,6], Yanina García Skabar[5], Paula Maldonado[5], Gimena Casaretto[5,6], Shigenori Otsuka[7], Arata Amemiya[7], Renato Pajarola[8], Takemasa Miyoshi[7]

[1]Universidad de Buenos Aires, Facultad de Ciencias Exactas y Naturales, Departamento de Ciencias de la Atmósfera y los Océanos. Buenos Aires, Argentina [2]CONICET – Universidad de Buenos Aires. Centro de Investigaciones del Mar y la Atmósfera (CIMA). Buenos Aires, Argentina [3]CNRS – IRD – CONICET – UBA. Instituto Franco-Argentino para el Estudio del Clima y sus Impactos (IRL 3351 IFAECI). Buenos Aires, Argentina. [4]Instituto de Modelado e Innovación Tecnológica, CONICET-UNNE, Corrientes, Argentina. [5]Servicio Meteorológico Nacional, Buenos Aires, Argentina. [6]Consejo Nacional de Investigaciones Científicas y Técnicas, Buenos Aires, Argentina. [7]RIKEN Cluster for Pioneering Research, Kobe, Japan. [8]University of Zürich, Zurich, Switzerland.

OBJETIVES

Extreme meteorological events associated with deep moist convection pose significant societal risks, emphasizing the need for advanced technologies to anticipate such events. This study focuses on improving data assimilation techniques to increase the forecast accuracy of deep convection events.

MODEL DESCRIPTION

Idealized experiments are conducted using the N-variable Lorenz model (L96), simulating damped-forced nonlinear advection dynamics over a 1-dimensional cyclic domain. Model equations are integrated using a Runge-Kutta scheme with a time step of 0.025 time units. The model forcing is set to $F = 8$ and the number of state variables is $N_x = 40$. Observations are simulated from the nature run using a predefined observation operator ($h(x)$) emulating radar reflectivity given by:

$$h(x) = \begin{cases} 0 & \text{if x < 5.0} \\ 10.0 \log_{10}(c(x-5.0)^{1.75} + 1.0) & \text{if x} \geq 5.0 \end{cases}$$

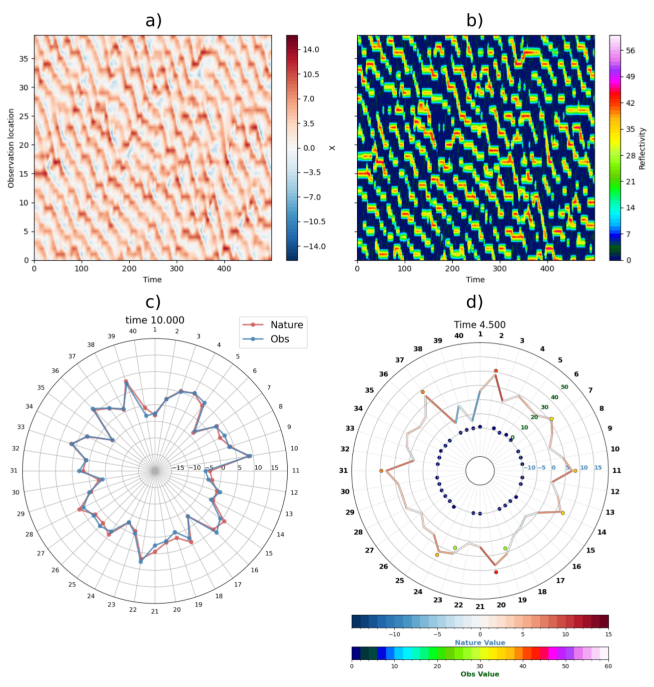

Figure 1. (a) shows the model solution over a time frame of 200 time units, (b) shows the evolution resulting from the application of h(x) at each model grid point.(c) Polar view of the state, (d) polar view in the operator space.

METHODS

The study uses the Local Ensemble Transform Kalman Filter (LETKF) to assimilate the observations. In this work we used the tempered LETKF, an iterative version of the filter associated with strongly nonlinear observation operators [Kurosawa and Poterjoy, 2021]. The tempered LETKF is described by the following algorithm:

Algorithm 1: Tempered LETKF Algorithm

Input: X^f, y_o, α

$X^{(0)} = X^f$

for $i = 1$ ***to*** N_α **do**

  for $n = 1$ ***to*** N_e **do**

    $Y_n^{(i-1)} = h\left(x^{(i-1,n)}\right) - \overline{y}^{(i-1)}$

  for $l = 1$ ***to*** N_x **do**

    $R_{loc}(l) = \rho_{loc}(l) \circ \left(\frac{R}{\alpha_i}\right)$

    $\tilde{P}^{(i)} = \left[(N_{ens}-1)I + \left(Y^{(i-1)}\right)^T R_{loc}^{-1} Y^{(i-1)}\right]^{-1}$

    $\overline{x}^{(i)}(l) =$
    $\overline{x}^{(i-1)}(l) + X_l^{(i-1)} \tilde{P}^{(i)} \left(Y^{(i-1)}\right)^T R_{loc}^{-1}\left(y_o - \overline{y}^{(i-1)}\right)$

    $X_l^{(i)} = X_l^{(i-1)} (N_{ens}-1)\left(\tilde{P}^{(i)}\right)^{\frac{1}{2}}$

$\overline{x}^a = \overline{x}^{(N_\alpha)}$

$X^a = X^{(N_\alpha)}$

Where N_α is the number of steps or parts in which the likelihood is factorized and α_i must satisfy the following condition:

$$\sum_{i=1}^{N_\alpha} \alpha_i = 1$$

Different choices are possible for the α_i. In this work, we propose the following form:

$$\alpha_i = \frac{\alpha_i'}{\sum_{i=1}^{N_\alpha} \alpha_i'} \quad \text{where} \quad \alpha_i' = e^{\frac{N_\alpha \alpha_s}{i}}$$

When the parameter $\alpha_s = 0$, α_i values are equal, and the observation error is the same at each iteration of the tempered-LETKF. The larger the α_s, the smaller the first α_i, resulting in a larger observation error at the first tempering iteration. This means that in the initial iterations, a relatively smaller portion of the information from the observations is assimilated.

SINGLE OBSERVATION EXPERIMENT

In these simple experiments we compare we assimilate a single observation with a nonlinear observation operator assuming a Gaussian prior. The particle filter posterior is used in this case as a reference. The posterior of the ETKF and tempered ETKF are compared, being the last one the one closer to the particle filter posterior (Figure 2)

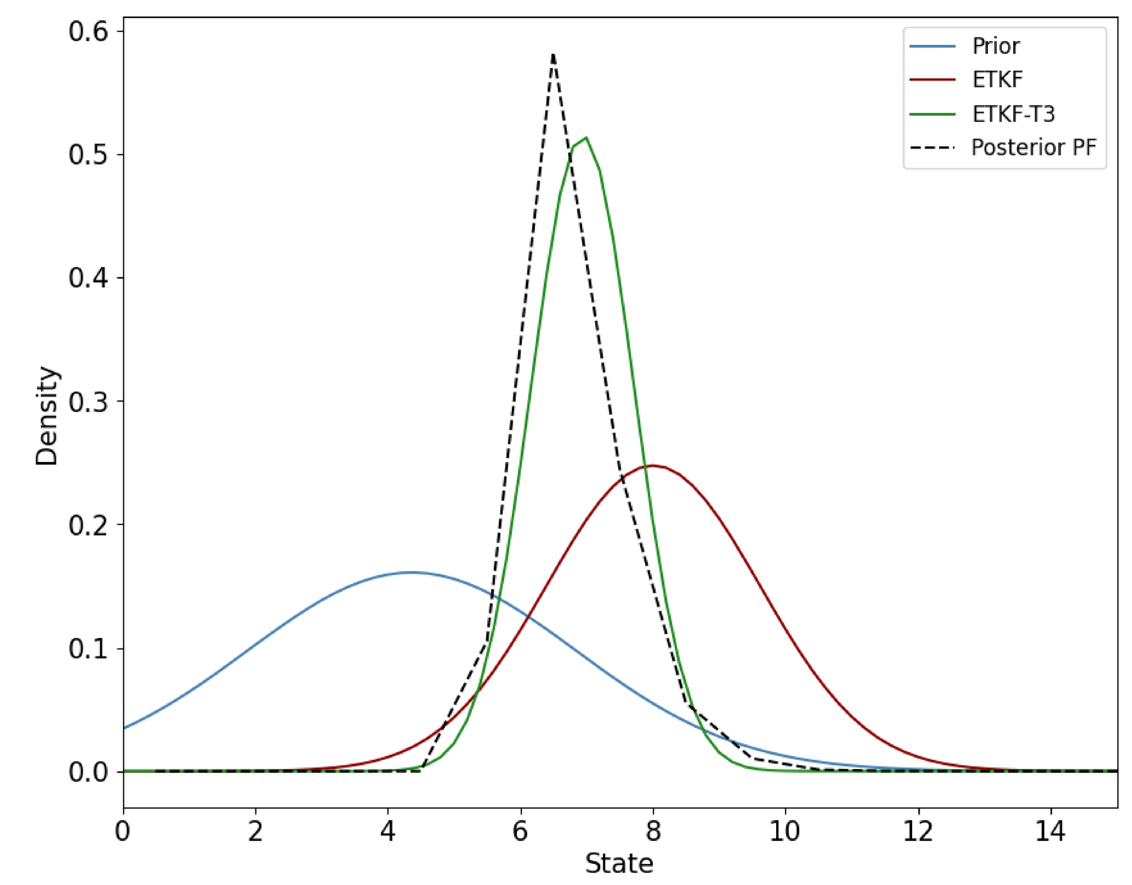

Figure 2. Probability density function for the prior specific concentration (blue line), the ETKF posterior (red line), the ETKF-T3 posterior o ETKF with 3 iterations (magenta line), and the importance sampling particle filter (black dashed line).

LORENZ-N ASSIMILATION EXPERIMENTS

Observations are assimilated using LETKF and tempered LETKF. Hereafter, we refer to the tempered versions with 2 and 3 iterations as LETKF-T2 and LETKF-T3, respectively. Experiments are conducted across different observation error levels to evaluate algorithm performance.

Our results, shown in Figure 3, indicate that the tempered LETKF consistently performs better than the LETKF, particularly when the observation error is low. This improvement is due to the iterative update approach used by the tempered LETKF, which effectively reduces the negative impacts caused by non-linear observation operators.

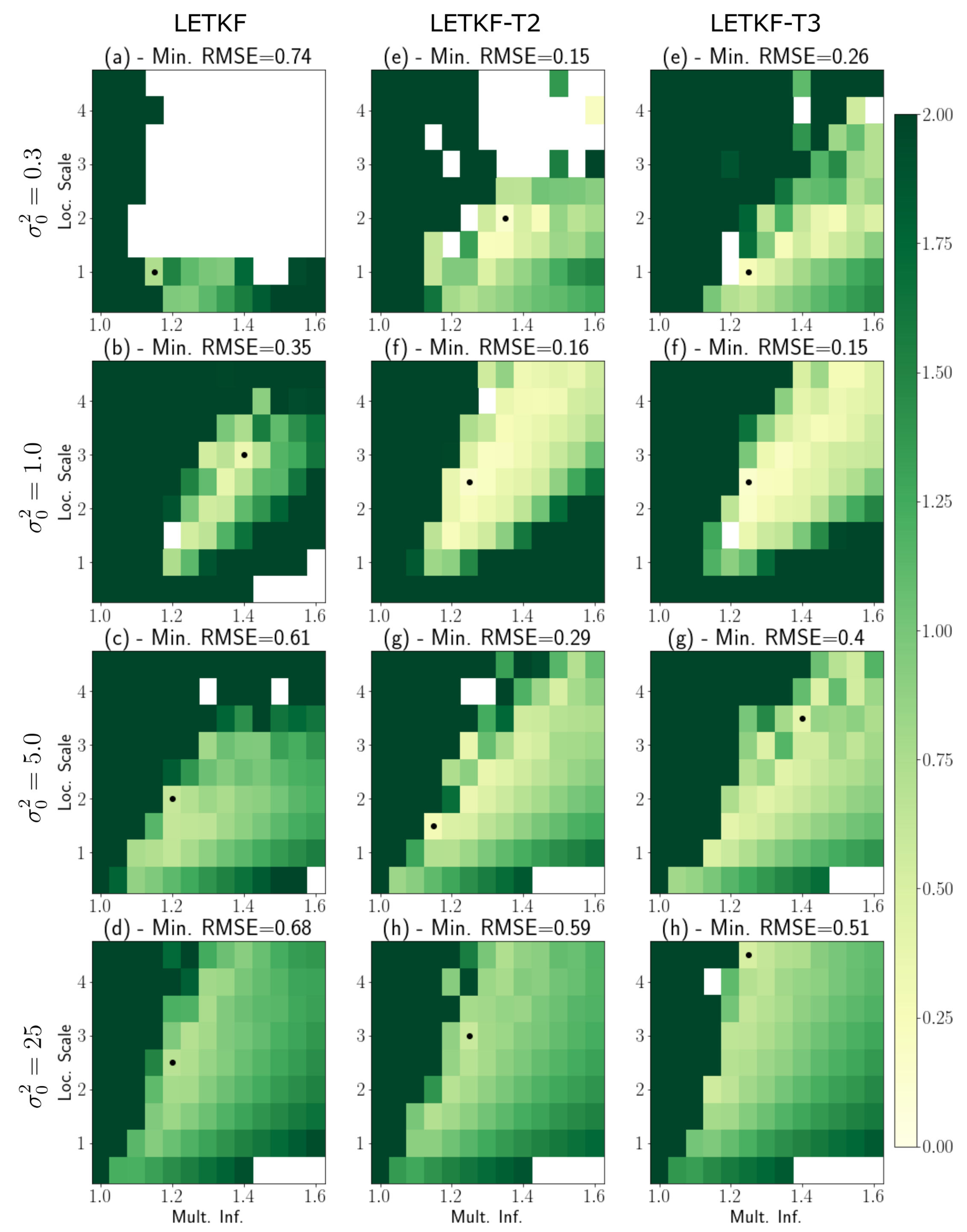

Figure 3. Time-averaged analysis RMSE as a function of the inflation factor (x-axis) and localization scale (y-axis) for different observation errors (σ_0^2) and number of iterations for the LETKF. The black dots indicate the location of the minimum RMSE for each case. Observation density = 1, observation frequency every 4 time steps, 20 ensemble members, and $\alpha_s = 2$.

In Figure 4 it can be observed that, although in all cases the tempered LETKF outperforms the LETKF, α_s can have a significant impact on the magnitude of the improvement. In this case, there is a tendency to see better results with $\alpha_s = 1$ and $\alpha_s = 2$. However, this is not always the case in other scenarios with different observation error and/or observation density. Also, the inflation and localization range explored may be too short in some of the scenarios.

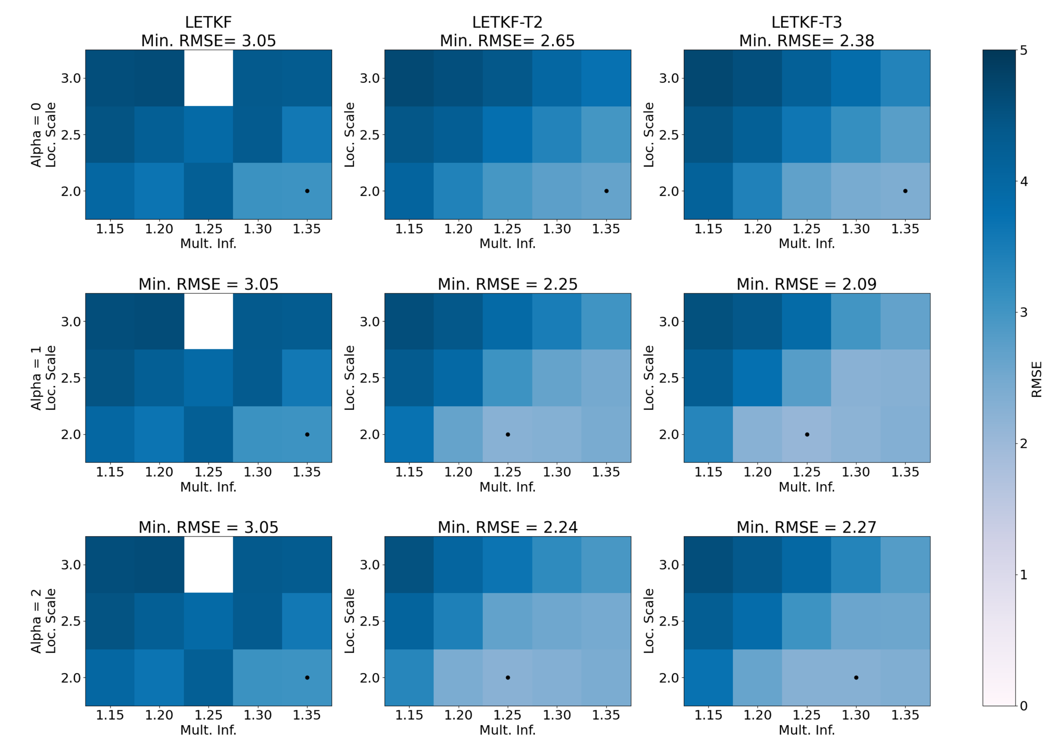

Figure 4. Time-averaged analysis RMSE as a function of the inflation factor (x-axis) and localization scale (y-axis) for different α_s and number of iterations for the LETKF. The black dots indicate the location of the minimum RMSE for each case. Observation density = 0.5, observation frequency every 8 time steps, 20 ensemble members, and $\sigma_0^2 = 5$.

We performed an experiment to evaluate the impact of tempering for different ensemble sizes. Figure 5, shows the analysis errors for ensemble sizes of 10, 20 and 40 members, and different number of tempering iterations. Overall, the larger the ensemble, the better the performance of the filter as expected. The impact of the tempering is significant independently of the ensemble size. This is consistent with the idea that tempering helps in the handling of nonlinearities in the observation operator, which can not be improved by the increase of the ensemble size.

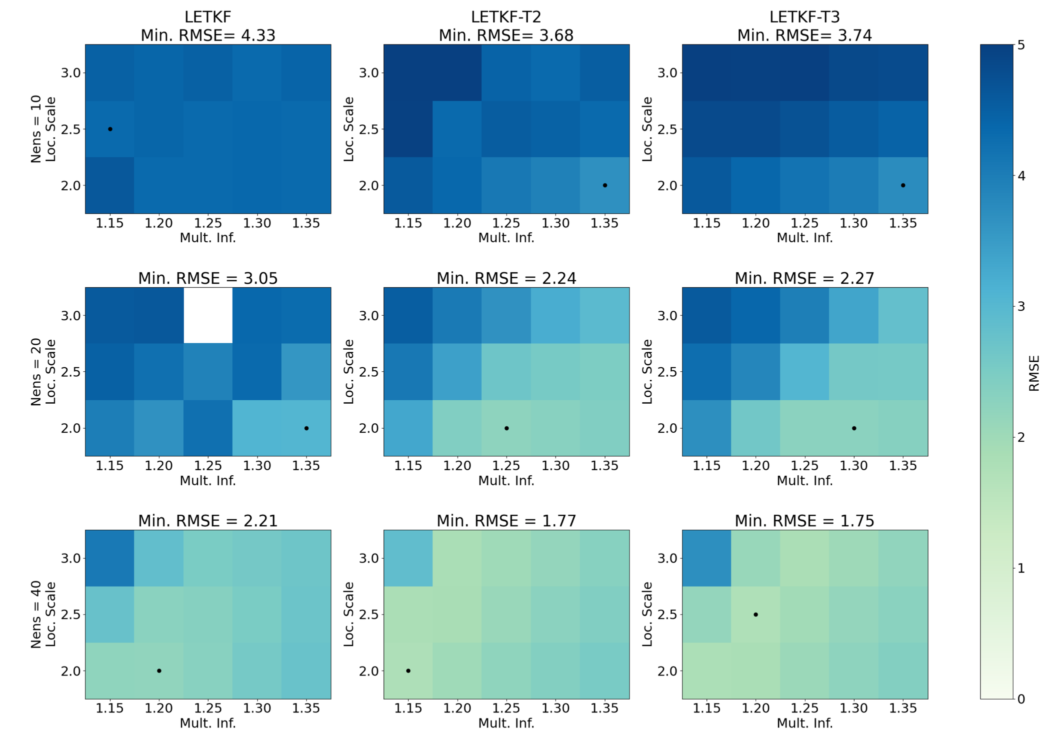

Figure 5. Time-averaged analysis RMSE as a function of the inflation factor (x-axis) and localization scale (y-axis) for different ensemble sizes and number of iterations for the LETKF. The black dots indicate the location of the minimum RMSE for each case. Observation density = 0.5, observation frequency every 8 time steps,$\alpha_s = 2$, and $\sigma_0^2 = 5$.

CONCLUSIONS

- The tempered LETKF improves the analysis accuracy with non-linear observation operators.
- The impact of the tempered LETKF is larger for smaller observation errors. This is an interesting property which may depend on the particular form of the observation operator.
- The distribution of the observation error among different tempering steps may have an impact on the performance of the filter.
- Current research is focused on evaluating the impact of tempered LETKF on convective scale radar data assimilation.

ACKNOWLEDGEMENTS

- SNF SPIRIT PROJECT: "UnWeather Vizard: Uncertainty Visualization and Analysis of High-Resolution Numeric Weather Forecasts"
- This study is conducted under the PREVENIR project under the Science and Technology Research Partnership for Sustainable Development (SATREPS) program jointly funded by the Japan International Cooperation Agency (JICA) and the Japan Science and Technology Agency (JST).

REFERENCES

A. Carrassi, M. Bocquet, L. Bertino, and G. Evensen. Data assimilation in the geosciences: An overview of methods, issues, and perspectives. *Wiley Interdisciplinary Reviews: Climate Change*, 9(5):e535, 2018.

K. Kurosawa and J. Poterjoy. Data assimilation challenges posed by nonlinear operators: A comparative study of ensemble and variational filters and smoothers. *Monthly Weather Review*, 149(7): 2369–2389, 2021.

*jorge.gacitua@cima.fcen.uba.ar